Mechanical Dissipation Below 1 μHz with a Cryogenic Diamagnetic Levitated Micro-Oscillator

Yingchun Leng[ORCID],[1] Rui Li[ORCID],[2,3,4] Xi Kong,[1] Han Xie[ORCID],[1] Di Zheng,[1] Peiran Yin[ORCID],[1] Fang Xiong,[1] Tong Wu[ORCID],[1] Chang-Kui Duan,[2,3,4] Youwei Du[ORCID],[1,5] Zhang-qi Yin,[6] Pu Huang[ORCID],[1,*] and Jiangfeng Du[2,3,4,†]

[1]*National Laboratory of Solid State Microstructures and Department of Physics, Nanjing University, Nanjing 210093, China*

[2]*Hefei National Laboratory for Physical Sciences at the Microscale and Department of Modern Physics, University of Science and Technology of China, Hefei 230026, China*

[3]*CAS Key Laboratory of Microscale Magnetic Resonance, University of Science and Technology of China, Hefei 230026, China*

[4]*Synergetic Innovation Center of Quantum Information and Quantum Physics, University of Science and Technology of China, Hefei 230026, China*

[5]*Collaborative Innovation Center of Advanced Microstructures and Jiangsu Key Laboratory for Nano Technology, Nanjing 210093, China*

[6]*Center for Quantum Technology Research and Key Laboratory of Advanced Optoelectronic Quantum Architecture and Measurements (MOE), School of Physics, Beijing Institute of Technology, Beijing 100081, China*

Ultralow-dissipation mechanical systems play an important role in metrology and exploring macroscopic quantum phenomena. Here we report a diamagnetic levitated micromechanical oscillator operating at 3 K with measured dissipation down to 0.59 μHz and a quality factor up to 2×10^7. This mechanical system achieves the lowest dissipation among the state-of-the-art microscale and nanoscale mechanical systems reported to date, with orders-of-magnitude reduction over other systems based on different principles. The cryogenic diamagnetic levitated oscillator is applicable on a wide range of mass, making it a good candidate system for ultrasensitive measurements of both force and acceleration. By virtue of the strong magnetic gradient, this system is potentially capable of studying quantum spin mechanics.

I. INTRODUCTION

Microscale and nanoscale mechanical systems have been developed as force sensors to detect different types of weak physical quantities, such as charge, spin, and mass [1–3]. Recently they have been considered as a potential tool to explore fundamental physics, such as dark-matter models [4–6], wave-function-collapse models [7–12], corrections to Newtonian gravity [13,14], and high-frequency gravitational waves [15]. To achieve a sufficiently high signal-to-noise ratio, the target signal should be greater than the noise level of the mechanical sensor, which is characterized by noise power density. On one hand, the noise power density of force is given by

$$S_{FF}(\omega_0) = 4m\gamma k_B T, \qquad (1)$$

where γ is the mechanical dissipation rate and k_B is the Boltzmann constant. The mechanical system can achieve high force sensitivity by reduction of the oscillator mass m even at room temperature [16]. On the other hand, the noise power density of acceleration is given by

$$S_{aa}(\omega_0) = \frac{4\gamma k_B T}{m}. \qquad (2)$$

To increase the acceleration sensitivity, it is necessary to increase the oscillator mass. Therefore, it is always beneficial to reduce the dissipation rate γ and temperature T to achieve high force and acceleration sensitivity.

Besides applications in metrology, ultralow dissipation is crucial for studying quantum phenomena at the macroscopic scale using microscale and nanoscale mechanical systems [17,18]. To realize and control a macroscopic quantum state, such as a spatial superposition, we have to suppress the thermal decoherence of the mechanical system. The thermal decoherence rate of a finite-temperature oscillator $\gamma_{\text{th}} = \bar{n}\gamma$, where $\bar{n} = k_B T/\hbar\omega_0$ is the thermal

*hp@nju.edu.cn
†djf@ustc.edu.cn

average phonon number [19]. To maintain a quantum superposition state within one oscillation period, the following relation holds:

$$\frac{\omega_0^2}{\gamma} > \frac{k_B T}{\hbar}. \qquad (3)$$

The term on the left-hand side is the product of the oscillator resonant frequency ω_0 and the quality factor $Q = \omega_0/\gamma$, known as the $\omega_0 Q$ product [19]. A lower temperature and a lower mechanical dissipation rate γ are always beneficial to maintain a better quantum coherent state.

For a solid-state mechanical oscillator in a high vacuum, the dissipation comes mainly from the direct coupling between the oscillator and the substrate, which is inversely proportional to the oscillator's mass. So it is challenging to achieve very low mechanical dissipation for small oscillators. Efforts have been made to achieve lower dissipation, such as optimizing the material [20,21], geometry [23], and strain [22]. Dissipation down to the scale of millihertz has been reported [22]. For an ultralight mechanical oscillator made of one-dimensional or two-dimensional materials, the lowest dissipation reported is 11 Hz with $m = 10^{-18}$ g [24].

A levitated mechanical oscillator in an ultrahigh vacuum achieves much lower dissipation [25]. Recently, optical levitation in a high vacuum [26–28] achieved about 10 μHz, and an electric trap [29] achieves about 81 μHz. Typically, those reported optical and electrical levitated oscillators work at room temperature, which limits their performance. Magnetic levitated oscillators, on the other hand, with no input energy, are especially suitable to work at low temperature. There are two types of magnetic levitated oscillators: Meissner levitated oscillators [30,31] and diamagnetic levitated oscillators [32,33]. Meissner levitated oscillators below 10 K were demonstrated recently [30,31], and achieved mechanical dissipation of approximately 10 μHz. However, a diamagnetic levitated oscillator working at low temperature has not been demonstrated [32–35].

Here we report a diamagnetic levitated microscale mechanical oscillator at low temperature. A diamagnetic microsphere with $m = 270$ pg is stably levitated in a magnetogravitational trap. An ultralow dissipation $\gamma/2\pi = 0.59 \pm 0.1$ μHz is observed at the resonant frequency 11.7 Hz, achieving a quality factor $Q = (2.0 \pm 0.4) \times 10^7$. Such dissipation is more than 10^3 times lower than that achieved with traditional solid-state oscillators [20–23], 10^1–10^3 times lower than that reported with optical levitated oscillators [26–28], Meissner levitated oscillators [30,31], and electrical levitated oscillators [29], and reduced by about 1 order of magnitude with respect to room-temperature diamagnetic levitated mechanical oscillators [32–35]. The mechanical dissipation achieved is even lower than that obtained with a state-of-the-art milligram-scale pendulum oscillator with mass more than 7 orders of magnitude larger [36,37]. The performance of this system as a force sensor or acceleration sensor is evaluated and its potential applications to realize quantum spin-mechanics systems are discussed.

II. EXPERIMENTAL SYSTEM

The experimental setup is shown in Fig. 1. A magnetogravitational trap is placed in a cryogen-free and high-vacuum cryostat. A specially designed spring-mass suspension system [Fig. 1(a)] is used to isolate the strong vibration generated by the cryostat [38,39]. The suspension structure consists of three stages, with each stage corresponding to a suspension load mass as well as a characteristic frequency. The designed isolation at a frequency of 8 Hz is 54 dB and is expected to be better at the resonant frequency of the diamagnetic levitated micromechanical oscillator (see Table I for parameters of the suspension structure).

The magnetogravitational trap is similar to the one used at room temperature [33] but with modifications of the geometry. The magnetic field is generated by a set of Sm-Co magnets with octagonal bilayer geometry as shown in Fig. 1(b). The oscillator is made of polyethylene glycol, which is loaded into the trap as a liquid microsphere by a homebuilt nebulizer at room temperature. The charge on the microsphere is eliminated by a standard procedure [33]. After pumping of the sample chamber to obtain a vacuum, the system is cooled and the oscillator becomes solid during the cooling process. The sample chamber is then maintained at 3 K during the experiment. The temperature of the magnetogravitational trap, due to its weak thermal connection to the cold plate of the sample chamber, has a higher temperature of about 7 K.

To obtain the position and the dynamics of the levitated microsphere, a weak 633-nm laser beam with power less than 50 μW is sent into the chamber via a single-mode fiber and is loosely focused on the microsphere [40,41]. The light scattered from the microsphere is collected vertically via the lens and the cryostat windows. An avalanche-photodiode detector is used to realize feedback cooling and excitation of the oscillator. Firstly, the intensity of scattered light, corresponding to the real time-information of the microsphere position, is measured by the avalanche-photodiode detector. Secondly, the signal is amplified and sent to a computer. The oscillation amplitude and phase at the resonant frequency are calculated. Then a program-based feedback circuit starts to control the current of a magnetic coil near the microsphere, which generates a weak magnetic field. Combined with the magnetic field gradient of the magnetogravitational trap, a feedback force is applied to the microsphere. A CMOS camera is used to record the absolute position of the microsphere. Figures 1(c) and 1(d) show typical images of the excited
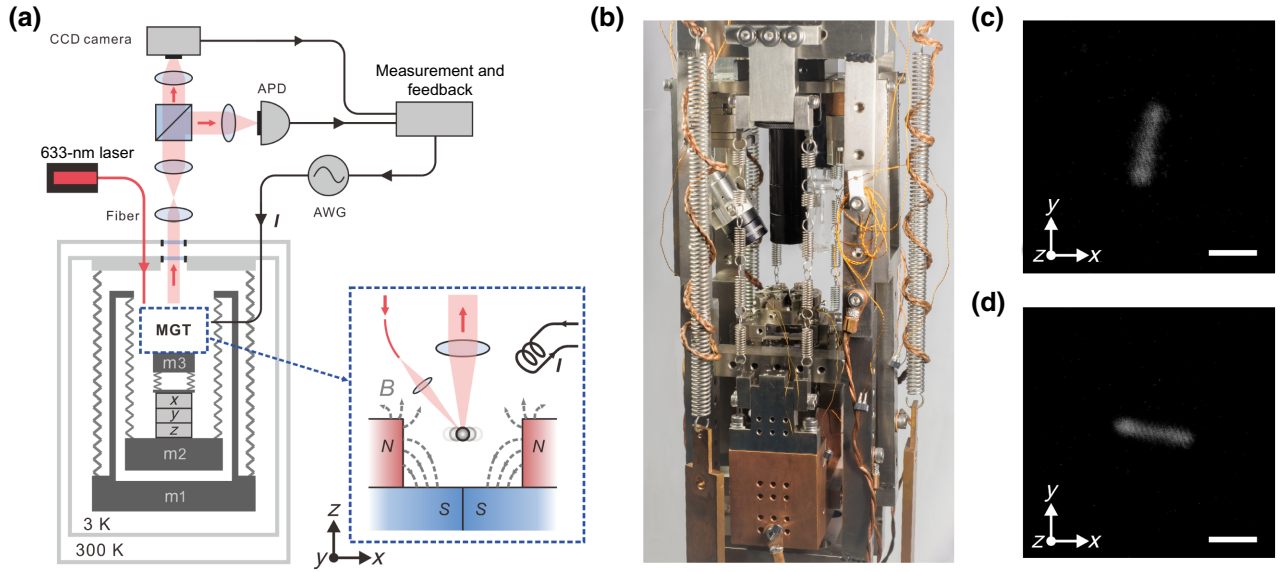
FIG. 1. Experimental setup. (a) The magnetogravitational trap (MGT) is placed on the three-stage spring-mass suspension system, which is used to isolate the external vibration. The whole structure is mounted inside the chamber of a cryostat. A 633-nm laser beam reaches the sample chamber through a fiber and is focused loosely on the microsphere. The piezoelectric positioners are used to control the position of the trap so that the scattered light can be collected via the lens. A CMOS camera is used to record the position of the microsphere, and an avalanche-photodiode detector (APD) is used to measure the real-time intensity of the scattered light, which is used as feedback to cool or excite the motion of the microsphere via the magnetic force of the magnetic field generated by a small coil near the MGT. (b) The spring-mass suspension structure and the MGT, where soft copper braids are used to realize thermal connection between different suspension stages. (c),(d) Snapshots of the excited motion of the microsphere corresponding to two oscillation modes of different resonant frequencies (mode 1, 11.7 Hz, mode 2, 8.4 Hz) in the x-y plane, where the exposure time is 200 ms, much longer than the oscillation period. The scale bar corresponds to 30 μm. AWG, arbitrary-waveform generator; m1 mass 1; m2, mass 2; m3, mass 3.

motion of the microsphere corresponding to two resonant modes.

III. MEASUREMENT METHOD AND RESULTS

The mechanical dissipation rate is obtained by our measuring the energy autocorrelation function $\langle X(t)^2 X(0)^2 \rangle$. The motion equation of the mechanical oscillator at resonant frequency $\omega_0/2\pi$ is

$$m\ddot{x} + m\gamma\dot{x} + m\omega_0^2 x + m\epsilon x^3 = F_{\text{fluc}}(t), \qquad (4)$$

TABLE I. Designed parameters of the vibration-isolation system. The characteristic frequency f_{char} is the mass-spring suspension resonant frequency in the vertical direction (z axis), which is significantly larger than the frequency in the horizontal direction (x, y), and the isolation is characterized by the attenuation of the square of the vibration amplitude response at a frequency of 8 Hz.

Stage	Mass (kg)	f_{char} (Hz)	Isolation (dB)
First	7	1.4	29
Second	1.6	2.5	19
Third	0.08	4.6	6

where γ is the dissipation rate, $m\epsilon x^3$ is the Duffing nonlinearity of the oscillator, and $F_{\text{fluc}}(t)$ is the total fluctuation force, including thermal fluctuation, external vibration, and so on. The motion can be written in the form $x(t) = X(t)\cos[\omega_0 t + \varphi(t)]$, where $X(t)$ and $\varphi(t)$ are the slow-varying amplitude and phase, respectively. There are several commonly used experimental methods to determine the dissipation rate γ. One method is to measure the frequency response of the system. For the harmonic oscillator, the full width at half maximum of the displacement power spectral density is $\gamma/2\pi$. However, because of nonlinearity, the full width at half maximum is significantly broadened, even in the presence of only the thermal fluctuation [26,33]. Thus a method to measure the decay of the energy autocorrelation $\langle X(t)^2 X(0)^2 \rangle$ that is insensitive to nonlinearity [42] is used in our experiment. The free decay of $X(t)^2$ is measured by our exciting the oscillator to initial amplitude $X(0)$, whose square is more than 10 times larger than the background stochastic motion $\langle X_{\text{ba}} \rangle^2$. The background stochastic motion $\langle X_{\text{ba}} \rangle^2$ is driven by the fluctuation force $F_{\text{fluc}}(t)$. The time evolution of $X(t)^2$ is then given by
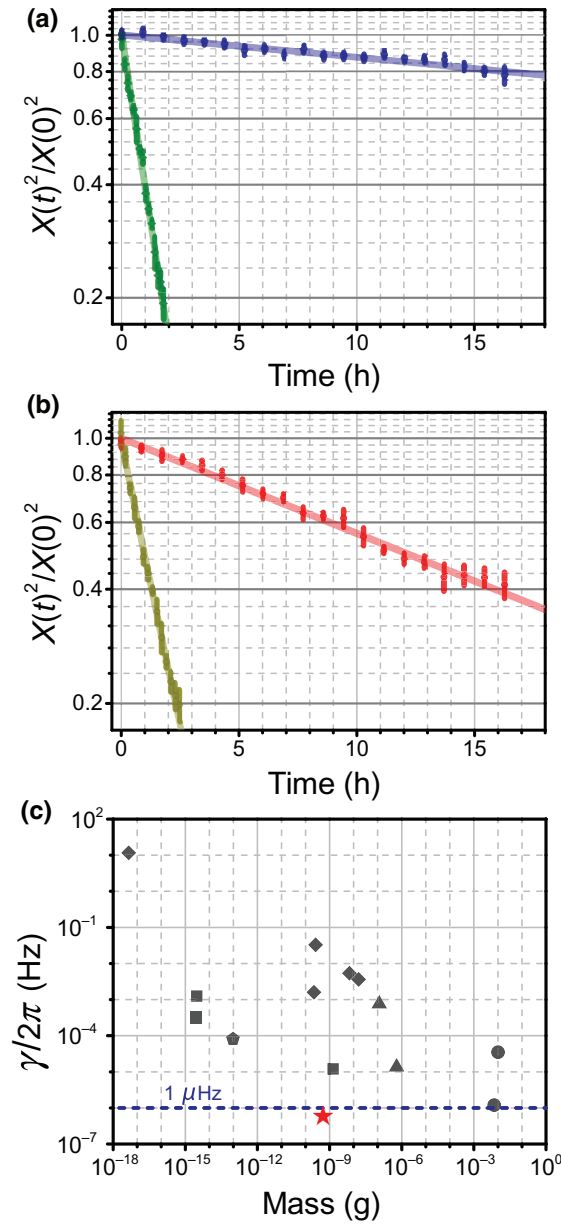
$$X(t)^2 = X(0)^2 e^{-t\gamma}, \qquad (5)$$

FIG. 2. Measured mechanical dissipation. (a) Logarithmic plot of the free ring-down normalized oscillation energy $X(t)^2/X(0)^2$ versus time for the oscillation mode of resonant frequency 11.7 Hz. Green and blue dots are results with statistic errors measured in a helium-gas environment and a vacuum without helium gas, respectively. Solid curves are fitted to the exponential decay [Eq. (5)]. (b) Same as (a) but for the oscillation mode of resonant frequency 8.4 Hz, with yellow for the helium-gas environment and red for a vacuum without helium gas. (c) The mechanical dissipation $\gamma/2\pi$ and the corresponding oscillator's mass for mechanical systems based on different principles. The blue dashed line indicates that the mechanical dissipation is 1 μHz. The red star corresponds to the 11.7-Hz mode in this experiment, rhombuses correspond to a solid-state oscillator [20–24], squares correspond to an optical levitated oscillator [26–28], the pentagon corresponds to an electrical levitated oscillator [29], triangles correspond to a Meissner levitated oscillator [30,31], and circles correspond to a milligram-scale pendulum oscillator [36,37].

with error less than a few percent [33,42]. In our experiment, $X(t)^2$ is obtained with the CMOS camera. The data processing is described in Supplemental Material [43]. Then the dissipation rate γ is obtained by our fitting the measured data with Eq. (5).

The diameter of the microsphere in the experiment is 7.8 ± 0.7 μm, which is obtained in advance from the thermal motion of the microsphere measured by the CMOS camera. The measurement is taken in a 2×10^{-4} mbar high-purity-helium-gas environment at room temperature. Then the system is cooled to 3 K and is ready for the dissipation measurement. Figures 2(a) and 2(b) show the free ring-down curve $X(t)^2/X(0)^2$ of oscillation modes 1 and 2 in helium gas of 2×10^{-6} mbar and a vacuum without helium gas of 3.3×10^{-7} mbar. The results are summarized in Table II. For the vibrational mode of the resonant frequency of 11.7 Hz (mode 1) in a vacuum without helium gas, we observe an ultralong damping time $\tau = 1/\gamma$ of 2.7×10^5 s (about 70 h), corresponding to mechanical dissipation $\gamma/2\pi = 0.59 \pm 0.11$ μHz and quality factor $Q = (2.0 \pm 0.4) \times 10^7$. The effective pressure around the microsphere is estimated to be on the order of 10^{-9} mbar with use of the dissipation of mode 1 [44] and the background gas is assumed to be residual helium gas at 3 K. Meanwhile, it has been observed that gas is probably not the primary limitation to dissipation at 10^{-10} mbar [32]. For the vibrational mode of the resonant frequency of 8.4 Hz (mode 2) in a vacuum without helium gas, the mechanical dissipation $\gamma/2\pi = 2.6 \pm 0.1$ μHz, which is about 4 times larger than the dissipation of mode 1. Further study is needed to reveal the mechanism of the difference. A possible origin may come from the boundary effect of residual helium gas [44–46] in the experiment. Figure 2(c) displays a comparison of our results with those obtained with previously reported microscale and nanoscale mechanical systems. It shows that our system has significantly lower dissipation over a wide range of mass, and is even comparable to the milligram-scale mechanical systems, whose mass is 7 orders of magnitude larger [36,37].

TABLE II. Measured mechanical dissipation at low temperature. The pressures of 2×10^{-6} and 3.3×10^{-7} mbar are measured at a side of the sample chamber at room temperature, corrsponding to the cases of helium gas being turned on and off, respectively. The diameter of the microsphere is 7.8 ± 0.7 μm and the corresponding mass is 270 ± 70 pg. The errors show the statistic deviations at the 95% confidence level.

Helium gas	Mode	$\gamma/2\pi$ (μHz)	Q ($\times 10^7$)
On (2×10^{-6} mbar)	1	41 ± 1	0.029 ± 0.001
	2	34 ± 1	0.025 ± 0.001
Off (3.3×10^{-7} mbar)	1	0.59 ± 0.11	2.0 ± 0.4
	2	2.6 ± 0.1	0.34 ± 0.02

IV. DISCUSSION AND SUMMARY

The potential performance of our diamagnetic levitated oscillator used for force and acceleration sensing can be evaluated from the dissipation rate achieved in our experiment. The sensitivity of a force or acceleration sensor is given by Eq. (1) or Eq. (2), respectively. In principle, a magnetogravitational trap can levitate particles over a very wide range of mass from 10^{-14} g [33] to 10^{-3} g [35]. Figure 3 shows the estimated force and acceleration sensitivity at 3 K corresponding to this experiment, and 10 mK which can be reached with a commercial dilution refrigerator. If the magnetic field gradient G is taken as 10^4 T/m [32], the force sensitivity is enough to detect a single electron spin by following the standard procedure [2] when the oscillator's mass is less than 1×10^{-7} g at 3 K. A single proton spin is also detectable when the oscillator's mass is less than 10^{-11} g at 10 mK. In addition, for a mass of 10^{-7} g the acceleration sensitivity is $\sqrt{S_{aa}(\omega_0)} < 10^{-10} g_0/\sqrt{\text{Hz}}$ ($g_0 = 9.8$ m/s^2) at 3 K, reaching the sensitivity of the state-of-the-art method [47].

Now we estimate the performance for studying the macroscopic quantum process with our system by assuming an oscillator resonant frequency $\omega_0/2\pi \simeq 100$ Hz [32] and temperature $T = 10$ mK. We find that $\omega_0 Q/2\pi \simeq 10^{10}$ Hz $\gg k_B T/2\pi\hbar$ and Eq. (3) is well satisfied. Therefore, the quantum coherence of the system could last for multiple oscillation periods. Moreover, it is interesting to realize quantum spin-mechanics dynamics [48,49]

with our system. Considering the interaction with an electron spin, the spin-mechanical coupling strength $\lambda = G x_{\text{ZPL}} \mu_e/\hbar$, where $x_{\text{ZPL}} = \sqrt{\hbar/m\omega_0}$ is the zero-point motion and μ_e is the electron spin magnetic moment. For an oscillator with $m = 10^{-13}$ g and $G = 10^4$ T/m, the coupling strength is $\lambda/2\pi \simeq 10$ kHz, which is 4 orders of magnitude larger than the decoherence rate $1/T_2$ of the electron spin at low temperature [50], and 4 orders of magnitude larger than the thermal decoherence rate γ_{th} of the oscillator. The cooperativity C here is $\lambda^2 T_2 Q\hbar/k_B T \simeq 10^8$, which marks the onset of highly coherent quantum effects. There are potential technical challenges to achieve these goals. For example, under the high-vacuum and low-temperature conditions, the microsphere is likely to be heated by the continuous-wave laser, especially at 10 mK, leading to a higher effective center-of-mass temperature than in the sample chamber [51]. These detection challenges were disscussed in Ref. [52].

In summary, we report a realization of a cryogenic diamagnetic levitated micromechanical oscillator with a low dissipation value, which provides a way to achieve high-performance sensing and realize quantum control of macroscopic mechanical dynamics.
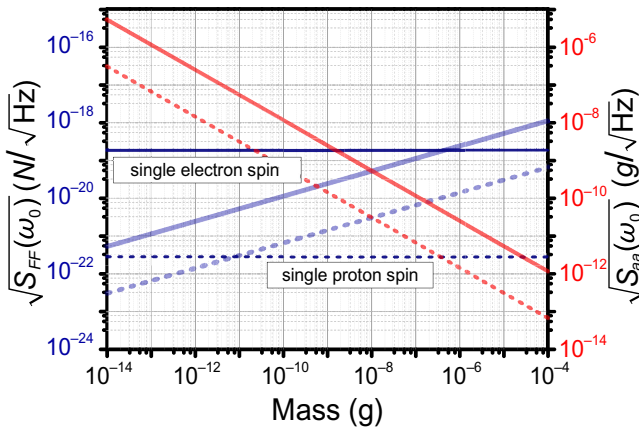
FIG. 3. Estimation for force and acceleration sensing. The force sensitivity (left axis) as a function of mass at an environmental temperature of 3 K (solid light-blue line) and 10 mK (dashed light-blue line). The force from a single electron spin (solid dark-blue line) and the force from a single proton spin (dashed dark-blue line) are shown for comparison. The right axis shows the acceleration sensitivity (red lines). Here we assume that dissipation is still dominated by gas. The experimentally measured dissipation $\gamma/2\pi = 0.59~\mu$Hz, diameter of the microsphere 7.8 μm, and magnetic gradient $G = 10^4$ T/m are adopted.

[1] A. N. Cleland and M. L. Roukes, A nanometre-scale mechanical electrometer, Nature (London) **392**, 160 (1998).

[2] D. Rugar, R. Budakian, H. J. Mamin, and B. W. Chui, Single spin detection by magnetic resonance force microscopy, Nature (London) **430**, 329 (2004).

[3] K. Jensen, K. Kim, and A. Zettl, An atomic-resolution nanomechanical mass sensor, Nat. Nanotechnol. **3**, 533 (2008).

[4] J. Manley, D. J. Wilson, R. Stump, D. Grin, and S. Singh, Searching for Scalar Dark Matter with Compact Mechanical Resonators, Phys. Rev. Lett. **124**, 151301 (2020).

[5] A. Kawasaki, Search for kilogram-scale dark matter with precision displacement sensors, Phys. Rev. D **99**, 023005 (2019).

[6] A. D. Rider, D. C. Moore, C. P. Blakemore, M. Louis, M. Lu, and G. Gratta, Search for Screened Interactions Associated with Dark Energy below the 100 μm Length Scale, Phys. Rev. Lett. **117**, 101101 (2016).

[7] S. L. Adler, Stochastic collapse and decoherence of a nondissipative forced harmonic oscillator, J. Phys. A-Math. **38**, 2729 (2005).

[8] M. Bahrami, M. Paternostro, A. Bassi, and H. Ulbricht, Proposal for a noninterferometric test of collapse models in optomechanical systems, Phys. Rev. Lett. **112**, 210404 (2014).

[9] S. Nimmrichter, K. Hornberger, and K. Hammerer, Optomechanical Sensing of Spontaneous Wave-Function Collapse, Phys. Rev. Lett. **113**, 020405 (2014).

[10] L. Diosi, Testing Spontaneous Wave-Function Collapse Models on Classical Mechanical Oscillators, Phys. Rev. Lett. **114**, 050403 (2015).

[11] A. Vinante, M. Bahrami, A. Bassi, O. Usenko, G. Wijts, and T. H. Oosterkamp, Upper bounds on spontaneous wave-function collapse models using Millikelvin-Cooled nanocantilevers, Phys. Rev. Lett. **116**, 090402 (2016).

[12] A. Vinante, R. Mezzena, P. Falferi, M. Carlesso, and A. Bassi, Improved noninterferometric test of collapse models using ultracold cantilevers, Phys. Rev. Lett. **119**, 110401 (2017).

[13] A. A. Geraci, S. B. Papp, and J. Kitching, Short-Range Force Detection Using Optically-Cooled Levitated Microspheres, Phys. Rev. Lett. **105**, 101101 (2010).

[14] R. S. Decca, D. Lopez, H. B. Chan, E. Fischbach, D. E. Krause, and C. R. Jamell, Constraining new forces in the casimir regime using the isoelectronic technique, Phys. Rev. Lett. **94**, 240401 (2005).

[15] A. Arvanitaki and A. A. Geraci, Detecting High-Frequency Gravitational Waves with Optically-Levitated Sensors, Phys. Rev. Lett. **110**, 071105 (2013).

[16] M. J. Biercuk, H. Uys, J. W. Britton, A. P. VanDevender, and J. J. Bollinger, Ultrasensitive detection of force and displacement using trapped ions, Nat. Nanotechnol. **5**, 646 (2010).

[17] V. B. Braginsky, V. P. Mitrofanov, and V. I. Panov, *Systems with Small Dissipation* (University of Chicago Press, Chicago, 1985).

[18] Y. Chen, Macroscopic quantum mechanics: Theory and experimental concepts of optomechanics, J. Phys. B **46**, 104001 (2013).

[19] M. Aspelmeyer, T. J. Kippenberg, and F. Marquardt, Cavity optomechanics, Rev. Mod. Phys. **86**, 1391 (2014).

[20] Y. Tao, J. M. Boss, B. A. Moores, and C. L. Degen, Single-crystal diamond nanomechanical resonators with quality factors exceeding one million, Nat. Commun. **5**, 3638 (2014).

[21] H. J. Mamin and D. Rugar, Sub-attonewton force detection at millikelvin temperatures, Appl. Phys. Lett. **79**, 3358 (2001).

[22] A. H. Ghadimi, S. A. Fedorov, N. J. Engelsen, M. J. Bereyhi, R. Schilling, D. J. Wilson, and T. J. Kippenberg, Elastic strain engineering for ultralow mechanical dissipation, Science **360**, 764 (2018).

[23] Y. Tsaturyan, A. Barg, E. S. Polzik, and A. Schliesser, Ultracoherent nanomechanical resonators via soft clamping and dissipation dilution, Nat. Nanotechnol. **12**, 776 (2017).

[24] J. Moser, A. Eichler, J. Güttinger, M. I. Dykman, and A. Bachtold, Nanotube mechanical resonators with quality factors of up to 5 million, Nat. Nanotechnol. **9**, 1007 (2014).

[25] D. E. Chang, C. A. Regal, S. B. Papp, D. J. Wilson, J. Ye, O. Painter, H. J. Kimble, and P. Zoller, Cavity optomechanics using an optically levitated nanosphere, Proc. Nat. Acad. Sci. U. S. A. **107**, 1005 (2009).

[26] J. Gieseler, L. Novotny, and R. Quidant, Thermal nonlinearities in a nanomechanical oscillator, Nat. Phys. **9**, 806 (2013).

[27] U. Delić, D. Grass, M. Reisenbauer, T. Damm, M. Weitz, N. Kiesel, and M. Aspelmeyer, Levitated cavity optomechanics in high vacuum, Quantum Sci. Technol. **5**, 025006 (2020).

[28] F. Monteiro, W. Li, G. Afek, C. L. Li, M. Mossman, and D. C. Moore, Force and acceleration sensing with optically levitated nanogram masses at microkelvin temperatures, Phys. Rev. A **101**, 053835 (2020).

[29] A. Pontin, N. P. Bullier, M. Toros, and P. F. Barker, Ultranarrow-linewidth levitated nano-oscillator for testing dissipative wave-function collapse, Phys. Rev. Res. **2**, 023349 (2020).

[30] J. Gieseler, A. Kabcenell, E. Rosenfeld, J. D. Schaefer, A. Safira, M. J. A. Schuetz, C. Gonzalez-Ballestero, C. C. Rusconi, O. Romero-Isart, and M. D. Lukin, Single-spin magnetomechanics with levitated micromagnets, Phys. Rev. Lett. **124**, 163604 (2020).

[31] A. Vinante, P. Falferi, G. Gasbarri, A. Setter, C. Timberlake, and H. Ulbricht, Ultralow mechanical damping with Meissner-Levitated ferromagnetic microparticles, Phys. Rev. Appl. **13**, 064027 (2020).

[32] B. R. Slezak, C. W. Lewandowski, J. F. Hsu, and B. D'Urso, Cooling the motion of a silica microsphere in a magneto-gravitational trap in ultra-high vacuum, New J. Phys. **20**, 063028 (2018).

[33] D. Zheng, Y. Leng, X. Kong, R. Li, Z. Wang, X. Luo, J. Zhao, C. K. Duan, P. Huang, J. Du, M. Carlesso, and A. Bassi, Room temperature test of the continuous spontaneous localization model using a levitated micro-oscillator, Phys. Rev. Res. **2**, 013057 (2020).

[34] P. Yin, R. Li, Z. Wang, S. Lin, T. Tian, L. Zhang, L. Wu, J. Zhao, C. K. Duan, P. Huang, and J. Du, Manipulation of a micro-Object using topological hydrodynamic tweezers, Phys. Rev. Appl. **12**, 044017 (2019).

[35] R. Nakashima, Diamagnetic levitation of a milligram-scale silica using permanent magnets for the use in a macroscopic quantum measurement, Phys. Lett. A **384**, 126592 (2020).

[36] K. Komori, Y. Enomoto, C. P. Ooi, Y. Miyazaki, N. Matsumoto, V. Sudhir, Y. Michimura, and M. Ando, Attonewton-meter torque sensing with a macroscopic optomechanical torsion pendulum, Phys. Rev. A **101**, 011802(R) (2020).

[37] S. B. Cataño-Lopez, J. G. Santiago-Condori, K. Edamatsu, and N. Matsumoto, High-Q milligram-scale monolithic pendulum for quantum-limited gravity measurements, Phys. Rev. Lett. **124**, 221102 (2020).

[38] See Supplemental Material at http://link.aps.org/supplemental/10.1103/PhysRevApplied.15.024061 for the vibration-isolation system.

[39] M. Pelliccione, A. Sciambi, J. Bartel, A. J. Keller, and D. Goldhaber-Gordon, Design of a scanning gate microscope for mesoscopic electron systems in a cryogen-free dilution refrigerator, Rev. Sci. Instrum. **84,** 033703 (2013).

[40] V. Jain, J. Gieseler, C. Moritz, C. Dellago, R. Quidant, and L. Novotny, Direct measurement of photon recoil from a levitated nanoparticle, Phys. Rev. Lett. **116,** 243601 (2016).

[41] C. Metzger, and K. Karrai, Cavity cooling of a microlever, Nature (London) **432,** 1002 (2004).

[42] B. C. Stipe, H. J. Mamin, T. D. Stowe, T. W. Kenny, and D. Rugar, Noncontact friction and force fluctuations between closely spaced bodies, Phys. Rev. Lett. **87,** 096801 (2001).

[43] See Supplemental Material at http://link.aps.org/supplemental/10.1103/PhysRevApplied.15.024061 for data-processing details.

[44] See Supplemental Material at http://link.aps.org/supplemental/10.1103/PhysRevApplied.15.024061 for the diameter of the microsphere.

[45] M. Defoort, K. J. Lulla, T. Crozes, O. Maillet, O. Bourgeois, and E. Collin, Slippage and Boundary Layer Probed in an Almost Ideal Gas by a Nanomechanical Oscillator, Phys. Rev. Lett. **113,** 136101 (2014).

[46] A. Cavalleri, G. Ciani, R. Dolesi, A. Heptonstall, M. Hueller, D. Nicolodi, S. Rowan, D. Tombolato, S. Vitale, P. J. Wass, and W. J. Weber, Increased Brownian Force Noise from Molecular Impacts in a Constrained Volume, Phys. Rev. Lett. **103,** 140601 (2009).

[47] C. Timberlake, G. Gasbarri, A. Vinante, A. Setter, and H. Ulbricht, Acceleration sensing with magnetically levitated oscillators above a superconductor, Appl. Phys. Lett. **115,** 224101 (2019).

[48] P. Rabl, P. Cappellaro, M. V. G. Dutt, L. Jiang, J. R. Maze, and M. D. Lukin, Strong magnetic coupling between an electronic spin qubit and a mechanical resonator, Phys. Rev. B **79,** 041302(R) (2009).

[49] Z. Q. Yin, T. Li, X. Zhang, and L. M. Duan, Large quantum superpositions of a levitated nanodiamond through spin-optomechanical coupling, Phys. Rev. A **88,** 033614 (2013).

[50] M. H. Abobeih, J. Cramer, M. A. Bakker, N. Kalb, M. Markham, D. J. Twitchen, and T. H. Taminiau, One-second coherence for a single electron spin coupled to a multi-qubit nuclear-spin environment, Nat. Commun. **9,** 2552 (2018).

[51] J. Millen, T. Deesuwan, P. F. Barker, and J. Anders, Nanoscale temperature measurements using non-equilibrium Brownian dynamics of a levitated nanosphere, Nat. Nanotechnol. **9,** 425 (2014).

[52] A. Vinante, A. Pontin, M. Rashid, M. Toros, P. F. Barker, and H. Ulbricht, Testing collapse models with levitated nanoparticles: Detection challenge, Phys. Rev. A **100,** 012119 (2019).